SWEPT-SOURCE OPTICAL COHERENCE TOMOGRAPHY ANGIOGRAPHY REVEALS CHORIOCAPILLARIS ALTERATIONS IN EYES WITH NASCENT GEOGRAPHIC ATROPHY AND DRUSEN-ASSOCIATED GEOGRAPHIC ATROPHY

HHS Public Access

Author manuscript

Retina. Author manuscript; available in PMC 2017 December 01.

Published in final edited form as:

Retina. 2016 December ; 36(Suppl 1): S2–S11. doi:10.1097/IAE.0000000000001287.

Swept source OCT angiography reveals choriocapillaris alterations in eyes with nascent geographic atrophy and drusen-associated atrophy

Eric M. Moult, BSc[1], **Nadia K. Waheed, MD MPH**[2,*], **Eduardo A. Novais, MD**[2,3], **WooJhon Choi, PhD**[1], **ByungKun Lee, MEng**[1], **Stefan B. Ploner, BSc**[1,4], **Emily Cole, BSc**[2], **Ricardo Louzada, MD**[2,5], **Chen D. Lu, MSc**[1], **Philip J. Rosenfeld, MD PhD**[6], **Jay S. Duker, MD**[2], and **James G. Fujimoto, PhD**[1]

[1]Department of Electrical Engineering and Computer Science, Research Laboratory of Electronics, Massachusetts Institute of Technology, Cambridge, MA

[2]New England Eye Center, Tufts Medical Center, Boston, Massachusetts

[3]Federal University of São Paulo, School of Medicine, São Paulo, Brazil

[4]Pattern Recognition Lab., Friedrich-Alexander University Erlangen-Nürnberg (FAU), Erlangen, Germany

[5]Federal University of Goiás, Goiânia, Brazil

[6]Department of Ophthalmology, Bascom Palmer Eye Institute, University of Miami Miller School of Medicine, Miami, Florida

Abstract

PURPOSE—To investigate choriocapillaris (CC) alteration in patients with nascent geographic atrophy (nGA) and/or drusen-associated atrophy (DAGA) using swept source optical coherence tomography (SS-OCT) angiography (SS-OCTA).

METHODS—A 1050 nm wavelength, 400 kHz A-scan rate SS-OCT prototype was used to perform volumetric SS-OCTA over 6 mm × 6 mm fields of view in patients with nGA and/or DAGA. The resulting OCT and OCTA data were analyzed using a combination of *en face* and cross-sectional techniques. Variable interscan time analysis (VISTA) was used to differentiate CC flow impairment from complete CC atrophy.

RESULTS—A total of seven eyes from six patients (mean age: 73.8 ± 5.7 years) were scanned. Seven areas of nGA and three areas of DAGA were identified. Analysis of cross-sectional OCT and OCTA images identified focal alterations of the CC underlying all seven areas of nGA and all three areas of DAGA. *En face* OCTA analysis of the CC revealed diffuse CC alterations in all eyes. VISTA processing suggested that the observed CC flow alterations predominantly corresponded to flow impairment rather than complete CC atrophy.

[*]**Corresponding Author/Reprint Requests**. Correspondence to Nadia K. Waheed MD MPH, New England Eye Center at Tufts Medical Center, 260 Tremont Street, Biewend Building, 9 - 11th Floor, Boston, MA 02116, T: 617-636-7950 / F: 617-636-4866, nadiakwaheed@gmail.com.

Conflicts of Interest: There are no conflicting relationships for any other author.

CONCLUSIONS—OCTA imaging of the CC revealed focal CC flow impairment associated with areas of nGA and DAGA, as well as diffuse CC flow impairment throughout the imaged field. *En face* OCT analysis should prove useful for understanding the pathogenesis of nGA and DAGA, and for identifying the formation of nGA and DAGA as endpoints in therapeutic trials.

Keywords

age-related macular degeneration (AMD); nascent geographic atrophy (nGA); drusen-associated atrophy (DAGA); choriocapillaris, optical coherence tomography (OCT); optical coherence tomography angiography (OCTA)

Introduction

Late age-related macular degeneration (AMD) is a leading cause of vision loss worldwide. Historically the exudative, or wet, form of late AMD, which is characterized by the formation of macular neovascularization (MNV), was responsible for the majority of AMD-related vision loss. However, with the introduction of vascular endothelial growth factor (VEGF) inhibitors, the prognosis for patients with exudative AMD has been improved, and the non-exudative form of late AMD, known as geographic atrophy (GA), may become a more important cause of severe vision loss in the future.[1]

GA is characterized by atrophy of the retinal pigment epithelium (RPE), photoreceptors, and choriocapillaris (CC).[2, 3] The CC, which is the monolayer capillary network of the choroidal blood supply, lies immediately beneath the RPE, abutting the Bruch's membrane, and is known to have a mutualistic relationship with the RPE.[2–5] While both the RPE and CC undergo atrophy in GA, there exists debate in the literature as to whether the CC or the RPE is the primary site of injury in GA.[3–6] With the aim of understanding AMD pathogenesis and developing endpoints for therapeutic trials, there has been considerable work on studying features of an earlier stage form of non-exudative AMD known as intermediate AMD. In particular, regions of nascent GA (nGA) associated with drusen have been shown to precede the formation of drusen-associated GA (DAGA).[7–10] DAGA has been defined using optical coherence tomography (OCT) imaging as areas of RPE and photoreceptor loss occurring in conjunction with increased light penetration or hyper-transmission below the Bruch's membrane.[7, 8] nGA has been defined on OCT as the subsidence of the outer plexiform layer (OPL) and inner nuclear layer (INL), and/or the presence of hyporeflective wedge-shaped bands.[7, 8] None of these definitions consider, at least directly, the vascular alterations of the CC. Given the hypothesized importance of the CC in the development of GA, it is likely valuable to develop criteria for assessing nGA and DAGA that include measures of CC alteration. However, developing such criteria requires imaging modalities that are capable of visualizing the CC vasculature.

While OCT has proved valuable for developing structural markers of AMD, traditional OCT technology does not readily visualize vascular features. Instead, dye-based methods such as fluorescein angiography (FA) and indocyanine green angiography (ICGA) have been used to study the vasculature of the retina and choroid. Unfortunately, dye-based techniques have a number of drawbacks, which include obfuscation of vascular detail due to dye-leakage, absence of depth-resolution, and adverse reactions to injected dyes; there are additional

complications when using dye-based methods to image the CC and choroid (Table 1). For these reasons, FA and ICGA imaging of the CC has played a limited role in studying non-exudative AMD. More recently, OCT angiography (OCTA) has shown great promise for visualizing the retinal and choroidal vasculature.[11–18] OCTA is a non-invasive, dye-free OCT-based imaging technique that allows for volumetric visualization of vasculature based on the motion-contrast generated by flowing erythrocytes. Compared to ICGA and FA, OCTA offers a number of advantages for imaging the CC and choroid (Table 1).

OCTA studies in AMD have primarily focused on the neovascular lesions occurring in exudative AMD, although imaging of the choriocapillaris and choroid in GA has been reported.[11, 22] Compared with imaging the retinal vasculature and MNV, imaging of the CC is more difficult due to the small dimensions of the CC vasculature, and the diminished OCT signal caused by RPE attenuation and signal roll-off.[23] It is likely a result of these difficulties that, to our knowledge, there have been no *in vivo* studies examining CC alterations in eyes with nGA and/or DAGA. Given the important role that the CC is suspected of playing in the development of GA, this void represents a significant gap in our understanding of disease progression, and hinders the development of endpoints for therapeutic trials. In this study, we use a long wavelength (1050 nm) ultrahigh-speed (400 kHz) SS-OCT system to perform OCT and OCTA imaging of eyes with nGA and/or DAGA. Using a combination of *en face* and cross-sectional analysis, we assess the association between regions of nGA and DAGA and those of CC alteration.

Methods

Patient Selection

The study was approved by the institutional review boards at the Massachusetts Institute of Technology and Tufts Medical Center. All participants were imaged in the ophthalmology clinic at the New England Eye Center at Tufts Medical Center. Written informed consent was obtained from all subjects before imaging. The research adhered to the Declaration of Helsinki and the Health Insurance Portability and Accountability Act. All subjects underwent a complete ophthalmic examination, including a detailed history, refraction, intraocular pressure measurement, anterior segment examination, and a dilated fundus examination by a general ophthalmologist or a retinal specialist at the New England Eye Center. Patients underwent color fundus photography, near-infrared reflectance (NIR) imaging, and fundus autofluorescence (FAF). Patients having nGA or DAGA were retrospectively identified from SD-OCT images obtained using the Cirrus HD-OCT (Carl Zeiss Meditec). Retrospective SS-OCT and SS-OCTA data, acquired from the system described in the following paragraph, were then examined for the identified patients.

SS-OCT and SS-OCTA Imaging

SS-OCT and SS-OCTA imaging was performed using a research prototype ultrahigh-speed SS-OCT system. As the system has been described in detail elsewhere,[24] only an overview is provided herein. Briefly, the system uses a 400 kHz vertical cavity surface emitting laser (VCSEL) centered at 1050 nm. The imaging range was ~2.1 mm in tissue, and the full-width-at-half-maximum (FWHM) axial and transverse resolutions in tissue were ~8–9 μm

and ~15 μm, respectively. The measured sensitivity was ~98 decibels using ~1.8 mW of incident power.

OCT and OCTA imaging was performed over 6 mm × 6 mm fields of view centered on the fovea, with 5 repeated B-scans taken at 500 uniformly spaced locations. Each B-scan consisted of 500 A-scans and the interscan time between repeated B-scans was ~1.5 ms, accounting for the mirror scanning duty cycle. A total of 5 × 500 × 500 A-scans were acquired per OCTA volume for a total acquisition time of ~3.9 s. The volumetric scan pattern yields isotropic transverse sampling of the retina at 12 μm over the 6 mm × 6 mm field of view. In order to compensate for patient motion, 2 orthogonally oriented volumes were acquired from each eye. These volumes were then registered and merged using a previously described algorithm.[25, 26] In addition to reducing motion artifacts, merging multiple datasets increases the signal-to-noise ratio in both the OCT and OCTA volumes.

OCTA images were formed by computing a decorrelation signal on a pixel-by-pixel basis. Images corresponding to different effective interscan times were formed using the previously described variable interscan time analysis (VISTA) algorithm.[11] Specifically, decorrelation of adjacent B-scans (i.e., 1↔2, 2↔3, 3↔4, and 4↔5) was used to generate OCTA data corresponding to a ~1.5 ms interscan time; decorrelation of every-other B-scan (i.e., 1↔3, 2↔4, and 3↔5) was used to generate OCTA data corresponding to a ~3.0 ms interscan time. Decorrelation signals corresponding to a given interscan time were averaged to improve the signal-to-noise ratio.

Image Analysis

Acquired SS-OCT and SS-OCTA data were flattened with respect to the Bruch's membrane by manually segmenting the Bruch's membrane on OCT B-scans. Segmentation of the Bruch's membrane is equivalent to the "RPE fit" segmentation performed by commercial SD-OCT systems. *En face* OCT projections, similar to the sub-RPE OCT slabs described by Yehoshua et al.,[27] were formed by computing the mean projection of the OCT signal, in the axial direction, from the Bruch's membrane to ~330 μm below the Bruch's membrane. *En face* OCTA projections were formed by computing the mean projection of the OCTA signal, in the axial direction, from the Bruch's membrane to ~90 μm below the Bruch's membrane. For reference, Figure 1 shows *en face* OCT and OCTA projections, along with OCTA B-scans in a normal eye. Further examples of OCTA in normal eyes are presented in Choi et al.[11] For the purposes of our research, nGA was identified on intensity *en face* OCT projections as any lesion showing increased light penetration over a region having a maximum linear dimension greater than 125 μm, but not evident on routine fundus imaging. OCT and OCTA B-scans intersecting the identified nGA and DAGA lesions were analyzed.

Results

A total of 7 eyes from 6 patients (mean age: 73.8 ± 5.7 years; 2 male and 4 female) were identified as having nGA and/or DAGA. From these 7 eyes, 7 nascent nGA lesions and 3 DAGA lesions were identified and analyzed (Figure 2 and Figure 3). All regions of nGA and DAGA showed marked CC alterations underlying the lesion. Furthermore, all 7 eyes exhibited diffuse CC alterations throughout the 6 mm × 6 mm field of view. Using the

VISTA algorithm, we found that the OCTA signal increased as the interscan time was increased, suggesting CC flow impairment rather than complete atrophy. However, different eyes, and different regions within the same eye, showed differing increases in OCTA signal when the interscan time was increased, which may be indicative of varying degrees of CC alteration.

Discussion

All of the examined areas of nGA and DAGA were shown to be associated with CC alterations. Furthermore, in all of the examined eyes we observed diffuse CC flow impairment occurring throughout the 6 mm × 6 mm field of view. These findings are important when considering the role that the CC and RPE may have in the development of GA, and, in particular, in determining where the original site of injury occurs in GA. As such, it is interesting to compare our finding to results from the histology literature. Histology studies by McLeod et al.[3, 28] found that CC loss was linearly related to RPE loss in regions of GA and that there was a 50% loss of CC density in regions of complete RPE atrophy. With no regions exhibiting complete CC atrophy, they concluded that the primary insult in GA was at the RPE. In an immunohistochemical study, Mullins et al.,[4] found that in eyes with early AMD, the CC vascular density was decreased when compared with normal eyes, and was inversely associated with the density of sub-RPE deposits. Furthermore, they reported that the density of ghost vessels, defined as vessels lacking a viable endothelium, was positively correlated with the density of sub-RPE deposits. A more recent study by Biesemeier et al.[6], using a combination of light and electron microscopy, observed CC loss occurring in regions underlying intact retina and RPE, and concluded that CC breakdown precedes RPE degeneration in AMD.

While comparison with histology studies helps to put our findings in context, there are fundamental differences between OCTA and histology that must be noted. First, OCTA images of the CC provide a direct marker for CC blood flow, rather than vascular structure. That said, certain histochemistry techniques, or examination of the endothelial ultrastructure using electron microscopy, are able to determine vessel viability and therefore give an indication of CC flow status.[4, 6, 29] Second, absence of an OCTA signal does not necessarily imply a complete absence of blood flow, but rather the absence of blood flow above the slowest detectable flow.[11] In our examination of eyes with nGA and/or DAGA using the VISTA algorithm, we noted significant increases in OCTA signal in most, but not all, areas, which suggests that the CC is predominantly impaired, rather than completely atrophied, in eyes with nGA and/or DAGA.

It is also important to understand our results in the context potential future studies performed with commercially available OCTA systems. First, from Figure 2, it is clear that CC alterations are more apparent with the shorter, 1.5 ms, interscan time than the longer, 3.0 ms, interscan time. Thus, when imaged with current commercial OCTA systems, which typically have interscan times of ~5 ms, CC flow impairment may be less evident or may not appear at all. This underscores the importance of ensuring that the effects of different interscan times are understood when reporting OCTA findings. In addition to the shorter interscan time, our SS-OCT system uses a long, ~1050 nm, wavelength source. Because of its location

beneath the highly scattering and absorbing RPE, shorter, ~840 nm, wavelength systems, which include the current commercially available SD-OCT units, can have difficulty achieving adequate signal levels at the CC. The presence of drusen further exacerbates the problem. Furthermore, if SD-OCT systems are used in the standard imaging protocol whereby the neurosensory retina is located in the upper portion of the OCT B-scan and the choroid and CC are located in the lower portion, SD-OCT signal roll-off further degrades the signal from the CC. Longer wavelength SS-OCT systems are less affected by RPE attenuation and do not suffer from signal roll-off, making long wavelength SS-OCT ideal for CC imaging.[23, 30]

In this study we used a combination of *en face* projection and cross-sectional OCT and OCTA analysis. As summarized in Table 2, *en face* and cross-sectional techniques both have their advantages and their disadvantages. Thus, it is our opinion that the question of cross-sectional versus *en face* analysis is not an either-or one; rather, analysis is most effective when the two techniques are used in combination. In the future we expect such hybrid analysis to be facilitated by the usage of orthoplane viewers.

A complicating factor when analyzing the CC using either *en face* or cross-sectional OCTA is the presence of the larger underlying choroidal vessels (Figure 4). In particular, even if the CC is impaired, or altogether lost, it may appear to be present if there is underlying choroidal vasculature that lies close to the Bruch's membrane. This phenomenon is most apparent in the *en face* CC projections, where we see diffuse CC alteration overlaying the OCTA signal arising from the larger choroidal vasculature. The obvious solution to this problem is to reduce the depth over which the OCTA signal is projected, thereby including less of the deeper choroid. However, as previously mentioned, since the CC is extremely thin, reducing the projection range requires increasingly accurate segmentation, which is difficult to achieve in practice. Thus, there is a trade-off between viewing artifacts from segmentation inaccuracies versus viewing contaminating OCTA signals from underlying choroidal vasculature. In general, artifacts from the underlying choroidal vasculature are easier to interpret because the OCTA signal appears along continuous vessels; artifacts from segmentation inaccuracies will most likely be random and are therefore harder to identify. For this reason, when forming our *en face* OCTA projections, we opted to use a larger projection range than anatomically occupied by the CC. Regardless, it is clear that the presence of underlying choroidal vasculature poses a significant challenge to the development of quantitative measures of CC alteration. The same complication arises in the case of *en face* OCT analysis projection's brightness being influenced not only by the RPE and photoreceptor alterations but also by the number and sizes of the underlying choroidal vessels. Since the choroidal vasculature generally scatters and absorbs the OCT signal, the projections look darker than areas with similar RPE and photoreceptors but with fewer choroidal vessels. In general, we found the choroidal interference to be less of a problem in the case of *en face* OCT analysis than in *en face* OCTA analysis.

In addition to the underlying choroidal vasculature, overlying retinal vasculature can also complicate *en face* and cross-sectional OCTA analysis of the CC. As marked in Figure 1, decorrelation tails, also referred to as projection artifacts, can cause overlying retinal vasculature to appear in the CC OCTA images. These decorrelation tails mix with the OCTA

signal arising from the CC layer and can obfuscate CC alterations (see arrow heads in L2.5 and L2.6 of Figure 3). As with underlying choroidal vasculature, decorrelation tails from overlying retinal vasculature pose a significant challenge to the development of quantitative measures of CC alteration.

There are several important limitations that should be considered when interpreting the results of this study. First, the number of examined nGA and DAGA lesions is small, and we lack an age-matched cohort of normal patients for comparison. The latter point is a particularly important limitation as CC density has been observed to decrease as a function of age.[31] However, the CC in normals having a range of ages has been previously reported,[11] and neither focal nor diffuse alterations of the type seen in the nGA and DAGA patients of this study were observed. Furthermore, that focal CC alterations were spatially associated with regions of nGA and DAGA is further evidence of a connection between the observed CC alterations and nGA and DAGA. Another limitation of this study is the lack of quantitative assessment, which limits the clinical applicability of the results. As mentioned earlier, a combination of image processing limitations, in particular segmentation accuracy, along with OCTA artifacts makes quantitative analysis a challenging task.

In this study we used an ultrahigh speed SS-OCT system to perform OCT and OCTA imaging of eyes with nGA and/or DAGA. A combination of *en face* and cross-sectional techniques were used to analyze the OCT and OCTA data. In addition to observing focal regions of CC flow alteration underlying nGA and DAGA, we also observed diffuse CC flow impairment throughout the imaged field. Although this study is qualitative in nature, it serves as a starting point for developing quantitative markers for measuring AMD progression using OCT and OCTA imaging.

Acknowledgments

Financial Support: This work was in part supported by a grant from the Macula Vision Research Foundation, New York, National Institute of Health (NIH R01-EY011289-29A, R44-EY022864, R01-CA075289-16, FA9550-15-1-0473 and FA9550-12-1-0499). EAN and RNL are researchers supported by CAPES Foundation, Ministry of Education of Brazil, Brasilia, DF, Brazil.

Jay S. Duker is a consultant for and receives research support from Carl Zeiss Meditec and OptoVue. Nadia K. Waheed was a consultant for Iconic therapeutics, served the speaker's bureau for Thrombogenics, and received research support from Carl Zeiss Meditec, Inc. Philip J. Rosenfeld has received research funding and speaker fees from Carl Zeiss Meditec. James G. Fujimoto: Royalties from intellectual property owned by the Massachusetts Institute of Technology and licensed to Carl Zeiss Meditec Inc., Optovue Inc.; Stock options – Optovue Inc.

References

1. Rein DB, Wittenborn JS, Zhang X, et al. Forecasting age-related macular degeneration through the year 2050: The potential impact of new treatments. Archives of Ophthalmology. 2009; 127:533–540. [PubMed: 19365036]
2. Sarks JP, Sarks SH, Killingsworth MC. Evolution of Geographic Atrophy of the Retinal-Pigment Epithelium. Eye. 1988; 2:552–577. [PubMed: 2476333]
3. McLeod DS, Grebe R, Bhutto I, et al. Relationship between RPE and Choriocapillaris in Age-Related Macular Degeneration. Investigative Ophthalmology & Visual Science. 2009; 50:4982–4991. [PubMed: 19357355]

4. Mullins RE, Johnson MN, Faidley EA, et al. Choriocapillaris Vascular Dropout Related to Density of Drusen in Human Eyes with Early Age-Related Macular Degeneration. Investigative Ophthalmology & Visual Science. 2011; 52:1606–1612. [PubMed: 21398287]
5. Bhutto I, Lutty G. Understanding age-related macular degeneration (AMD): Relationships between the photoreceptor/retinal pigment epithelium/Bruch's membrane/choriocapillaris complex. Molecular Aspects of Medicine. 2012; 33:295–317. [PubMed: 22542780]
6. Biesemeier A, Taubitz T, Julien S, et al. Choriocapillaris breakdown precedes retinal degeneration in age-related macular degeneration. Neurobiology of Aging. 2014; 35:2562–2573. [PubMed: 24925811]
7. Wu Z, Luu CD, Ayton LN, et al. Optical Coherence Tomography-Defined Changes Preceding the Development of Drusen-Associated Atrophy in Age-Related Macular Degeneration. Ophthalmology. 2014; 121:2415–2422. [PubMed: 25109931]
8. Wu Z, Luu CD, Ayton LN, et al. Fundus Autofluorescence Characteristics of Nascent Geographic Atrophy in Age-Related Macular DegenerationFAF of Nascent Geographic Atrophy in AMD. Investigative Ophthalmology & Visual Science. 2015; 56:1546–1552. [PubMed: 25678689]
9. Ouyang Y, Heussen FM, Hariri A, et al. Optical Coherence Tomography–Based Observation of the Natural History of Drusenoid Lesion in Eyes with Dry Age-related Macular Degeneration. Ophthalmology. 2013; 120:2656–2665. [PubMed: 23830761]
10. Christenbury JG, Folgar FA, O'Connell RV, et al. Progression of Intermediate Age-related Macular Degeneration with Proliferation and Inner Retinal Migration of Hyperreflective Foci. Ophthalmology. 2013; 120:1038–1045. [PubMed: 23352193]
11. Choi W, Moult EM, Waheed NK, et al. Ultrahigh-Speed, Swept-Source Optical Coherence Tomography Angiography in Nonexudative Age-Related Macular Degeneration with Geographic Atrophy. Ophthalmology. 2015; 122:2532–2544. [PubMed: 26481819]
12. Choi W, Mohler KJ, Potsaid B, et al. Choriocapillaris and choroidal microvasculature imaging with ultrahigh speed OCT angiography. Plos One. 2013; 8:e81499. [PubMed: 24349078]
13. Braaf B, Vienola KV, Sheehy CK, et al. Real-time eye motion correction in phase-resolved OCT angiography with tracking SLO. Biomed Opt Express. 2013; 4:51–65. [PubMed: 23304647]
14. Braaf B, Vermeer KA, Vienola KV, et al. Angiography of the retina and the choroid with phase-resolved OCT using interval-optimized backstitched B-scans. Optics Express. 2012; 20:20516–20534. [PubMed: 23037099]
15. Braaf B, Vermeer KA, Sicam VADP, et al. Phase-stabilized optical frequency domain imaging at 1-mu m for the measurement of blood flow in the human choroid. Optics Express. 2011; 19:20886–20903. [PubMed: 21997098]
16. Jia Y, Bailey ST, Wilson DJ, et al. Quantitative optical coherence tomography angiography of choroidal neovascularization in age-related macular degeneration. Ophthalmology. 2014; 121:1435–1444. [PubMed: 24679442]
17. Schwartz DM, Fingler J, Kim DY, et al. Phase-variance optical coherence tomography: a technique for noninvasive angiography. Ophthalmology. 2014; 121:180–187. [PubMed: 24156929]
18. Huang Y, Zhang Q, Thorell MR, et al. Swept-source OCT Angiography of the Retinal Vasculature using Intensity Differentiation Based OMAG Algorithms. Ophthalmic surgery, lasers & imaging retina. 2014; 45:382–389.
19. Bischoff P, Flower R. Ten years experience with choroidal angiography using indocyanine green dye: a new routine examination or an epilogue? Documenta Ophthalmologica. 1985; 60:235–291. [PubMed: 2414083]
20. Flower RW. Extraction of choriocapillaris hemodynamic data from ICG fluorescence angiograms. Investigative Ophthalmology & Visual Science. 1993; 34:2720–2729. [PubMed: 8344794]
21. Zhu L, Zheng Y, von Kerczek CH, et al. Feasibility of Extracting Velocity Distribution in Choriocapillaris in Human Eyes from ICG Dye Angiograms. Journal of Biomechanical Engineering. 2005; 128:203–209.
22. Jia Y, Bailey ST, Hwang TS, et al. Quantitative optical coherence tomography angiography of vascular abnormalities in the living human eye. Proceedings of the National Academy of Sciences. 2015; 112:E2395–E2402.

23. Unterhuber A, Povazay B, Hermann B, et al. In vivo retinal optical coherence tomography at 1040 nm-enhanced penetration into the choroid. Optics Express. 2005; 13:3252–3258. [PubMed: 19495226]

24. Choi W, Potsaid B, Jayaraman V, et al. Phase-sensitive swept-source optical coherence tomography imaging of the human retina with a vertical cavity surface-emitting laser light source. Optics Letters. 2013; 38:338–340. [PubMed: 23381430]

25. Kraus MF, Liu JJ, Schottenhamml J, et al. Quantitative 3D-OCT motion correction with tilt and illumination correction, robust similarity measure and regularization. Biomedical optics express. 2014; 5:2591–2613. [PubMed: 25136488]

26. Kraus MF, Potsaid B, Mayer MA, et al. Motion correction in optical coherence tomography volumes on a per A-scan basis using orthogonal scan patterns. Biomedical optics express. 2012; 3:1182–1199. [PubMed: 22741067]

27. Yehoshua Z, Garcia Filho CA, Penha FM, et al. Comparison of geographic atrophy measurements from the OCT fundus image and the sub-RPE slab image. Ophthalmic Surg Lasers Imaging Retina. 2013; 44:127–132. [PubMed: 23510038]

28. McLeod DS, Taomoto M, Otsuji T, et al. Quantifying Changes in RPE and Choroidal Vasculature in Eyes with Age-Related Macular Degeneration. Investigative Ophthalmology & Visual Science. 2002; 43:1986–1993. [PubMed: 12037009]

29. McLeod DS, Lutty GA. High-resolution histologic analysis of the human choroidal vasculature. Invest Ophthalmol Vis Sci. 1994; 35:3799–3811. [PubMed: 7928177]

30. Potsaid B, Baumann B, Huang D, et al. Ultrahigh speed 1050nm swept source/Fourier domain OCT retinal and anterior segment imaging at 100,000 to 400,000 axial scans per second. Opt Express. 2010; 18:20029–20048. [PubMed: 20940894]

31. Ramrattan RS, van der Schaft TL, Mooy CM, et al. Morphometric analysis of Bruch's membrane, the choriocapillaris, and the choroid in aging. Investigative Ophthalmology & Visual Science. 1994; 35:2857–2864. [PubMed: 8188481]

Summary Statement

Swept source OCT angiography reveals choriocapillaris alterations in eyes with nascent geographic atrophy and drusen-associated atrophy.

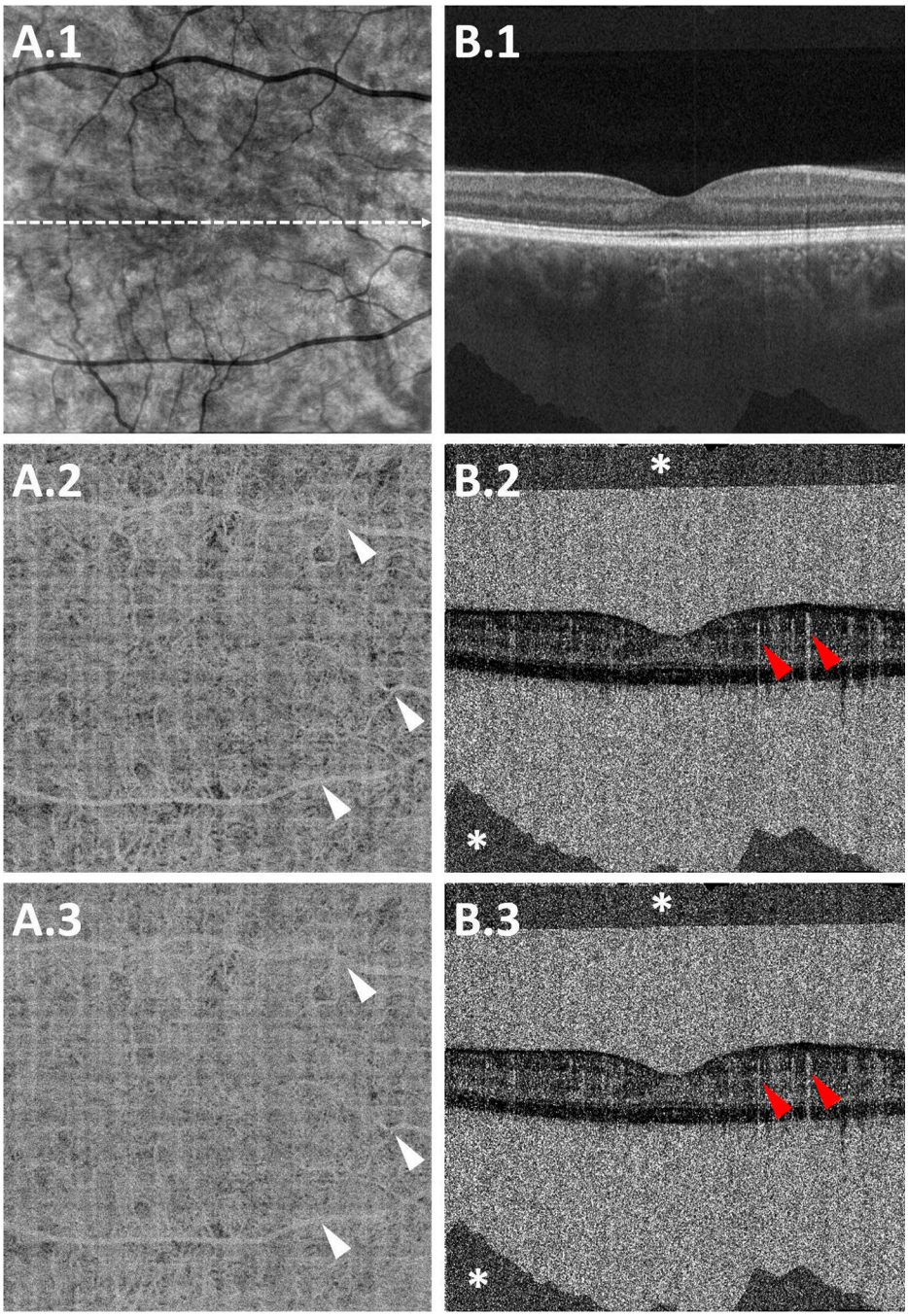

Figure 1.

En face and cross-sectional optical coherence tomography (OCT) and OCT angiography (OCTA) data from a 45 year old normal control. (A.1) *En face* mean projection of the OCT volume through the 330 μm immediately below the segmented Bruch's membrane. (A.2) *En face* mean projection of the ~1.5 ms interscan time OCTA volume through the ~90 μm immediately below the segmented Bruch's membrane. (A.3) *En face* mean projection of the ~3.0 ms interscan time OCTA volume over the same depths as in A.2. (B.1) OCT B-scan taken from the dashed white arrow in A.1. (B.2) ~1.5 ms interscan time OCTA B-scan taken

at the same location. (B.3) ~3.0 ms interscan time OCTA B-scan taken at the same location. Note that since the OCTA data are not thresholded, there is necessarily a high decorrelation signal in the regions of low OCT signal, in particular in the vitreous and deep choroid. The grid-like pattern that appears in the *en face* OCTA images A.2 and A.3, and consists of vertically and horizontally oriented stripes of relative brightness, is a residual motion artifact that is not completely eliminated in the process of merging two orthogonally acquired volumes. The brightness variation, marked with the asterisks, occurring in the OCTA B-scans is also an artifact of volume merging, occurring in regions only covered by one of the two orthogonally acquired volumes. Finally, note that OCTA decorrelation tails, also referred to as projection artifacts, are present in both the *en face* (white arrows) and cross-sectional (red arrows) OCTA images.

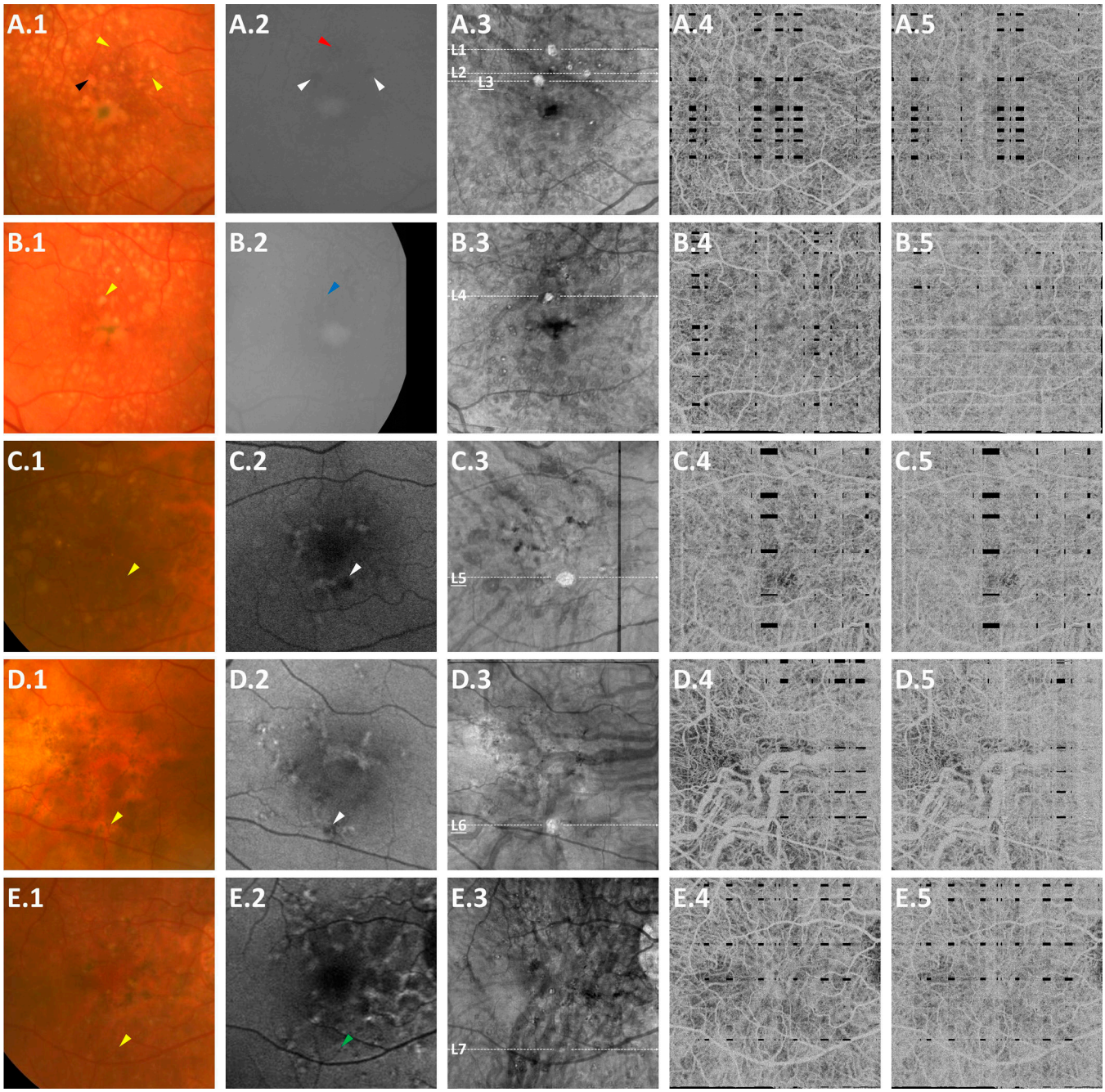

Figure 2.

This figure illustrates the diffuse CC flow impairment apparent in *en face* OCTA images of eyes with nGA and/or DAGA lesions. Note that the CC flow impairment is more apparent in the 1.5 ms interscan time OCTA (fourth row) than the 3.0 ms interscan time OCTA (fifth row). Focal, lesion-associated CC alteration is present, but only manifest underlying certain lesions (most prominently L1 and L5); focal CC alteration is most evident with cross-sectional analysis, as shown in Figure 3. (A.1–A.5) 65 year old male; (B.1–B.5) fellow eye of same patient; (C.1–C.5) 74 year old female; (D.1–D.5) 73 year old female; (E.1–E.5) 75 year old male. For each patient, the first column is the color fundus photograph, cropped

over the 6 mm × 6 mm region corresponding to the OCT field; the second column is the FAF, cropped over the 6 mm × 6 mm region corresponding to the OCT field; the third column is the *en face* mean projection of the OCT volume through the 330 μm immediately below the segmented Bruch's membrane; the fourth column is the *en face* mean projection of the ~1.5 ms interscan time OCTA volume through the ~90 μm immediately below the segmented Bruch's membrane; and the fifth column is the *en face* mean projection of the ~3.0 ms interscan time OCTA volume through the same depth. All OCT and OCTA images correspond to a 6 mm × 6 mm field of view. Note that the black rectangles appearing in the *en face* OCT and OCTA images are motion artifacts, and correspond to regions where there was no reliable OCT signal from either of the merged volumes. The black arrow head points to the lesion identified as having atrophy on fundus photography; yellow arrow heads point to lesions identified as having no atrophy on fundus photography. White arrow heads correspond to lesions identified as having hypo-autofluorescence on FAF; the red arrow head corresponds to the lesion identified as having mixed-autofluorescence on FAF; the green arrow head corresponds to the lesion identified as having hyper-autofluorescence on FAF; and the blue arrow head corresponds to the lesion identified as having normal autofluorescence on FAF. The dashed white arrows in the third column, labelled L1–L7, intersect the identified nGA and DAGA lesions, and are from where the cross-sectional images of Figure 3 were extracted. Underlined lettering indicates the DAGA lesions; the others are nGA lesions. Note that in (A–D).3, the nGA and DAGA lesions are easily visualized as a well-defined focal region of increased light penetration. In E.3, the lesion is still visible as an area of increased light penetration, but its contrast from the rest of the field is lower than in the other cases. In all cases, there is diffuse CC alteration. Furthermore, increasing the interscan time from ~1.5 ms to ~3.0 ms increases the OCTA signal in all cases, suggesting that we are observing CC flow impairment, rather than total CC atrophy.

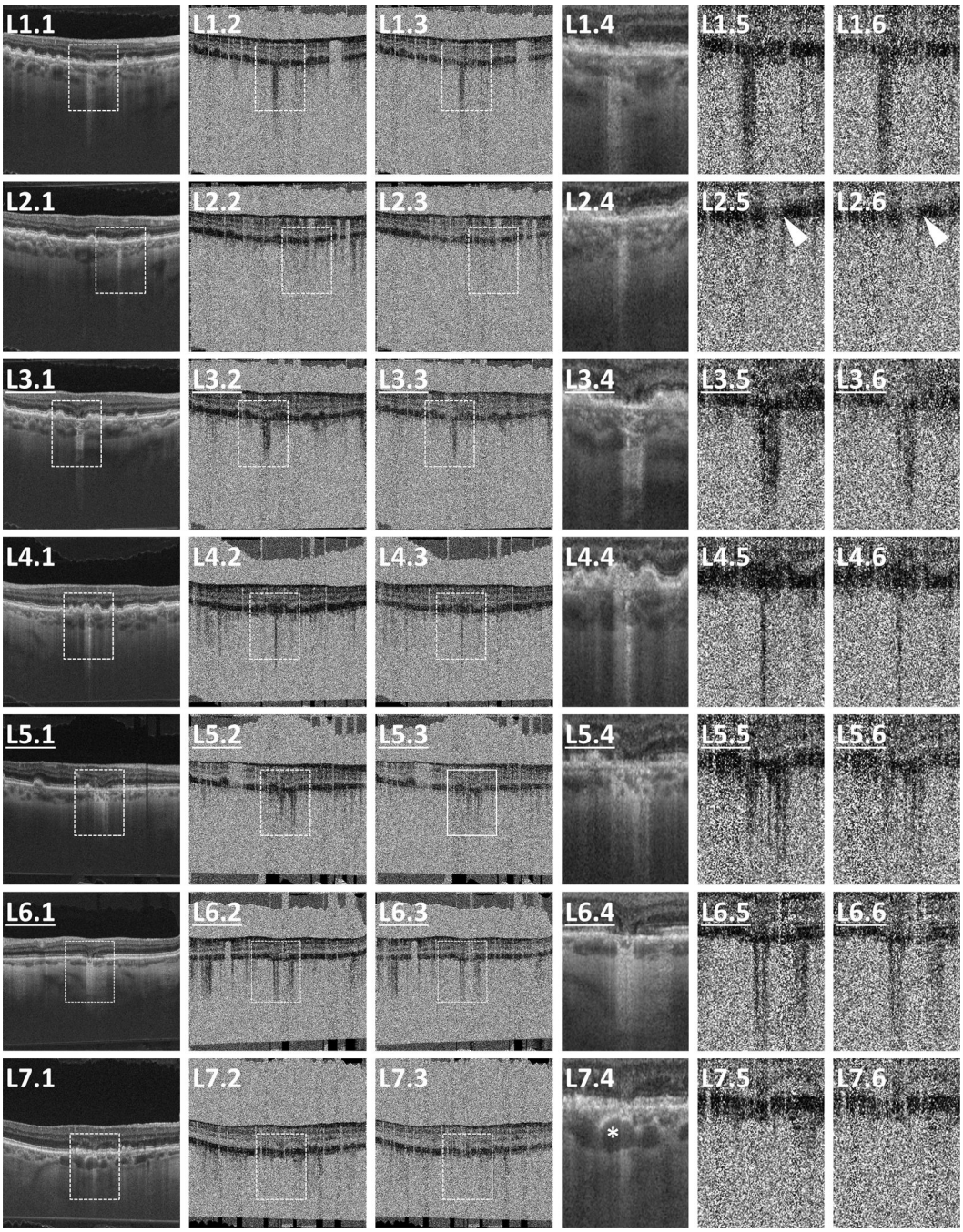

Figure 3.

This figure illustrates the focal CC flow impairment underlying nGA and DAGA lesions. Each row, L1–L7, was extracted from the corresponding dashed arrow in Figure 2. Underlined lettering indicates the DAGA lesions; the others are nGA lesions. The first column shows the OCT B-scan; the second the ~1.5 ms interscan time OCTA B-scan; and the third the ~3.0 ms interscan time OCTA B-scan. Columns four through six show enlargements of the dashed white boxes shown in columns one through three, respectively. Close examination of the OCTA cross-sections reveals low OCTA signal associated with the

regions of nGA and DAGA. Visualizing this alteration is complicated in L2 and L7. In L2, OCTA decorrelation tails from an overlying retinal vessel obfuscate the central region of the CC flow impairment; this can been seen by tracing down the decorrelation tail in L2.2, and L2.3, and by noting the characteristic decorrelation streak appearing in the RPE region, indicated by the arrowheads in L2.5 and L2.6. In the case of L7, we can see a larger choroidal vessel, indicated by the asterisk in L7.4, lying directly beneath the lesion of interest. This larger vessel causes an increase in the OCTA signal, limiting the depth persistence of the CC alteration to only a few pixels. Both of these complications are considered in more detail in the Discussion section of this paper.

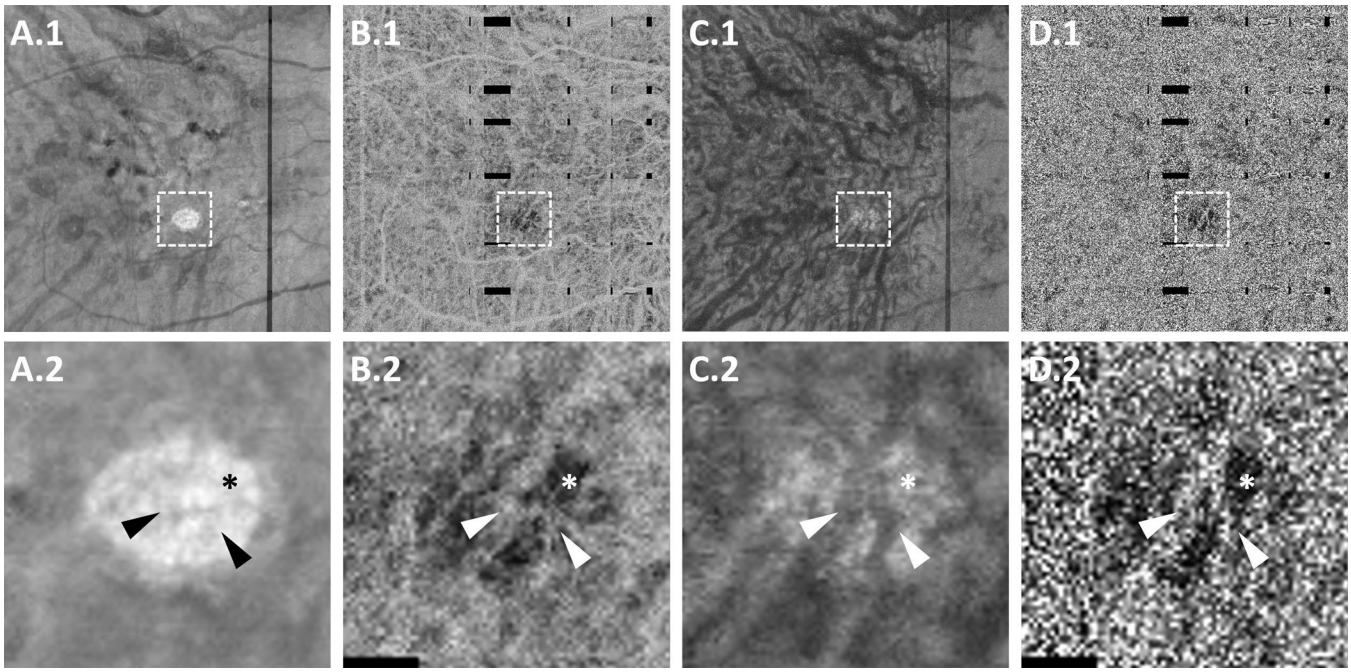

Figure 4.

This figure illustrates how underlying choroidal vasculature can complicate OCTA analysis of the CC. Top row corresponds to 6 mm × 6 mm *en face* OCT and OCTA images from the same eye as in Figure 2, row C; bottom row corresponds to enlargements of the dashed white boxes shown in the top row. (A) *En face* mean projection of the OCT volume through the 330 μm immediately below the segmented Bruch's membrane (same as Figure 2, subpanel C.3); (B) *en face* mean projection of the ~1.5 ms interscan time OCTA volume through the ~90 μm immediately below the segmented Bruch's membrane (same as Figure 2, subpanel C.4); (C) single, 4.4 μm *en face* slice of the OCT volume, located ~90 μm below the segmented Bruch's membrane; and (D) single, 4.4 μm *en face* slice of the ~1.5 ms interscan time OCTA volume, located ~90 μm below the segmented Bruch's membrane. In (B–D).2, two choroidal vessels are visible in the region underlying the lesion (arrow heads). These vessels are not visible in (A.2), underscoring that *en face* OCT projection is less influenced by the underlying choroidal vessels than *en face* OCTA projection. The asterisk marks an area of decreased OCTA signal.

Table 1

Summary of the advantages and disadvantages of FA, ICGA, and OCTA imaging of the CC.

	Advantages		Disadvantages	
FA	•	Can be used to study time dynamics and vascular leakage	•	Shorter excitation wavelength is largely blocked by the RPE
			•	Leakage of fluorescein from capillary fenestrations obscures choriocapillaris vasculature[19]
			•	Not depth resolved
			•	Requires specialized imaging protocol
ICGA	•	Can be used to study time dynamics and vascular leakage	•	Not depth resolved, making it difficult to separate the fluorescence signal generated by the larger choroidal vessels[19–21]
	•	Longer excitation wavelength penetrates the RPE	•	Requires specialized imaging protocol
	•	Higher bonding affinity of the ICG results in less dye leakage		
OCTA	•	Depth resolved	•	Does not capture time dynamics, vascular leakage
	•	Image wavelengths can penetrate through the RPE (especially with longer, 1050 nm, systems)		
	•	No obfuscation of vasculature from dye leakage		
	•	Can be acquired with standard OCT, allowing for simultaneous assessment of structure and flow		

Table 2

Summary of the advantages and disadvantages of the *en face* and cross-sectional techniques used in this study.

	Advantages		Disadvantages	
En face OCT projection	•	Enables rapid identification of nGA and DAGA lesions	•	Requires segmentation
	•	Has potential to be used to develop quantitative measures of RPE and photoreceptor alteration		
En face OCTA projection	•	Enables assessment of global and diffuse CC alteration	•	Requires segmentation
			•	Difficult to identify focal CC alterations associated with nGA and DAGA lesions
Cross-sectional OCT	•	Enables detailed examination of structural alterations occurring in nGA and DAGA (e.g., subsidence of the OPL/INL)	•	Data intensive and time-consuming to review large B-scan stacks
			•	Difficult to assess spatial extent of lesions
			•	Difficult to develop quantitative metrics of RPE and photoreceptor alteration
Cross-sectional OCTA	•	Can be used to assess spatial relationships between nGA and DAGA lesions and underlying CC alteration	•	Data intensive and time-consuming to review large B-scan stacks
			•	Difficult to assess global CC alteration
			•	Difficult to develop quantitative metrics of CC alteration